

Modeling fats, oil and grease deposit formation and accumulation in sewer collection systems

Roya Yousefelahiyeh, Christopher Cyril Sandeep Dominic and Joel Ducoste

ABSTRACT

Fats, oil and grease (FOG) deposits in sewer systems are responsible for approximately 25% of all annual line blockages in the United States and lead to the release of 3–10 million gallons of untreated wastewater to the surrounding environment. Considerable effort has been made to maintain the conveyance of wastewater by cleaning pipes that have a significant FOG deposit accumulation. Changes in the urban landscape from the addition or deletion of food service establishments (FSEs), however, may pose challenges in determining the location of these high accumulation zones. This research focuses on the development of a sewer collection system model that predicts high FOG deposit accumulation zones. Two collection systems were simulated to test the prediction capabilities of the tool and to assess how changes in the urban landscape affect the location of these accumulation zones. The numerical tool incorporates a mechanistic-based FOG deposit formation kinetic model. Results showed that the model predicts about 65% of the reported high FOG deposit accumulating zones. Simulations also showed significant changes in the location of these high FOG deposit accumulating zones from changes in the number and locations of FSEs and from FSE discharge and background wastewater flow variations.

Key words | FOG deposits, food service establishment, numerical modeling, sanitary sewer overflows, sewer collection system, wastewater conveyance

Roya Yousefelahiyeh
Christopher Cyril Sandeep Dominic
Joel Ducoste (corresponding author)
Department of Civil Construction and
Environmental Engineering,
North Carolina State University,
208 Mann Hall, Campus Box 7908, 2501 Stinson
Drive,
Raleigh,
NC 27695,
USA
E-mail: jducoste@ncsu.edu

INTRODUCTION

The detrimental effects of fats, oil and grease (FOG) deposits on sewer collection systems have been documented extensively. The EPA estimated that there are approximately 23,000 to 75,000 sanitary sewer overflows (SSOs) in the United States each year (US EPA 2004). Of these large numbers of SSOs, 47% of those that were caused by line blockages were associated with FOG accumulation in sewer lines (US EPA 2012). In a recent Australian study, one water utility company reported that 21% of all blockages were primarily due to FOG deposit accumulation (Mattsson *et al.* 2014).

FOG wastes are primarily composed of triglycerides, i.e., esters of glycerol and fatty acids, and are generated at

food service establishments (FSEs) as by-products of food preparation activities (Williams *et al.* 2012). In addition to FSEs, a significant contribution to FOG production may come from residential sources, specifically in areas with high population densities (Ducoste *et al.* 2009).

Since a major source of FOG is FSEs, the presence of FSEs at different locations may increase the risk of FOG deposit accumulation and the subsequent SSO if no maintenance is performed. The extent of FOG deposit accumulation within the collection system can vary spatially and depends on many factors, including but not limited to pipe structural condition, pipe deformation, accumulation of debris or root intrusion (Marlow *et al.*

2010; Dominic *et al.* 2013), partial or inadequate flows (Marlow *et al.* 2010), location and density of FSEs, multi-family dwellings and high rise buildings (Gray 2002; Mattsson *et al.* 2014), and corresponding kitchen practices and poorly maintained grease interceptors (Williams *et al.* 2012). To prevent excessive FOG deposits' accumulation and subsequent SSOs, pretreatment managers perform routine maintenance by identifying locations with high rates of FOG deposit accumulation and using high pressure jets to clean the partially clogged pipe segments. While pretreatment managers may be aware of current maintenance requirements of an existing sewer system, the spatial distribution of FOG deposits may change due to the changing urban landscape (i.e., changes in the number and location of FSEs) caused by ongoing revitalization of many urban centers across the United States. Prediction of the new high FOG deposit accumulation zones would require a model that simulates the transport of wastewater and the reaction process that describes how FOG deposits are formed.

Research studies have shown that FOG wastes may undergo alkali-driven hydrolysis which results in the production of free fatty acids (FFA) (Iasmin *et al.* 2014, 2016). Fatty acids, which are a major constituent of edible oils and fats (Ma & Hanna 1999; Canakci 2007; Williams *et al.* 2012), may also be released as a result of cooking processes (Canakci 2007) or microbial activity (Brooksbank *et al.* 2007).

Hydrolysis is the precursor of a saponification reaction by which FOG deposits are formed (He *et al.* 2011, 2013; Iasmin *et al.* 2014). Iasmin *et al.* (2016) proposed a mechanistic model that included alkali-driven hydrolysis of triglyceride based on mass action principles and were able to predict changes in the rate of formation of saponified solids under different experimental conditions. They studied the kinetics of FOG deposits' formation for two types of fat and two types of calcium sources under three pH and two temperature conditions. In their work, an aqueous solution of calcium chloride/calcium sulfate was prepared and brought down to room temperature (22–25 °C). The liquid/melted-solid fat (canola or beef tallow) was then added to the aqueous calcium solution and mixed for 8 hours under different pH (7 ± 0.5, 10 ± 0.5, and ≈14) and temperature conditions (25 and 45 °C). Samples were collected at

specific intervals and analyzed with Fourier transform infrared spectrometer for their spectral data. The experimental data were then compared to mechanistic and empirical models.

In Iasmin *et al.*'s (2016) model, the formation of FFAs from the hydrolysis of triglyceride was assumed to follow a one-step irreversible reaction process (Equation (1)). The rate of triglyceride hydrolysis was assumed to follow a fourth order reaction kinetics that was proportional to the presence of unreacted triglyceride and water in the system. FFA produced from triglyceride hydrolysis were consumed in a saponification reaction (Equation (2)) that followed a third order reaction kinetics in which two moles of FFA react with one mole of calcium ions to produce calcium-based fatty acid salts, i.e., calcium-based saponified solids. A first order reverse reaction kinetics for the possible destruction of the saponified solids was assumed in the saponification reaction (Iasmin *et al.* 2016). However, the rate of destruction was related to possible breakdown and/or dissolution of the saponified solids (i.e., solid phase to liquid phase) and was hypothesized to occur due to the intense mixing conditions in their test reactor (Iasmin *et al.* 2016):

Triglyceride (FOG) + 3 water



where k_T = reaction rate constant for the hydrolysis of triglyceride ($\text{L}^3 \text{ mol}^{-3} \text{ hr}^{-1}$), k_s = reaction rate constant for saponification of FFA and Ca^{2+} ($\text{L}^2 \text{ mol}^{-2} \text{ hr}^{-1}$), and k_d = reaction rate constant for breakdown and/or dissolution (solid phase to liquid phase) of the saponified solids (hr^{-1}).

Although the model described by Iasmin *et al.* (2016) was based on reactions between pure fats and calcium in the background wastewater (BGWW), it does provide an initial framework that could be used in a system-wide description of the sewer collection system. What is still missing, however, is a description of accumulating solids in any particular sewer pipe section.

In rheological experiments performed by [Iasmin *et al.* \(2014\)](#) on FOG deposits and calcium-based fatty acid salts, results showed that both calcium-based fatty acid salts and FOG deposits displayed rigid stability indicating their limited flow properties when adhered to the sewer wall. [Keener *et al.* \(2008\)](#) and [He *et al.* \(2011\)](#) showed that FOG deposits also demonstrated adhesive characteristics and can become securely bound to the interior pipe wall. The results of [Keener *et al.* \(2008\)](#), [He *et al.* \(2013\)](#), and [Iasmin *et al.* \(2014\)](#), clearly showed that FOG deposits, whether formed in the wastewater bulk solution or directly on the pipe wall, can accumulate along the pipe surface due to their rheological properties. Consequently, a mechanism must be developed that describes the FOG deposit adhesion process.

This research presents a model that describes the fate and transport of FOG deposits and their intermediates through the sewer collection system. To the authors' knowledge, no previous research on modeling FOG deposit accumulation in a system-wide sewer collection model has been performed. The model uses CITY DRAIN 2.0.3 ([Achleitner *et al.* 2007](#); [Achleitner 2008](#)), which is an open-source software integrated within MATLAB/Simulink, that monitors the locations with the highest rate of FOG deposits' accumulation at the pipe wall. These locations are addressed as 'hotspots' throughout this study and represent the highest risk of an SSO occurrence due to FOG deposit accumulation. The purpose of this model is to investigate the potential impact of changes in the number and location of FSEs on the predicted locations of hotspots. The goal of this research and model is to develop a predictive tool that pretreatment managers could use to assess future sewer maintenance requirements with respect to high FOG deposit accumulating pipe segments.

METHODS

CITYDRAIN 2.0.3 was used to model the sanitary sewer collection system. The graphical interface of CITYDRAIN includes various blocks representing straight pipes, mixers, and separators that make the user able to construct a model of an urban drainage system block by block.

Muskingum's method of flood routing

CITYDRAIN is based on Muskingum's equation of flood routing ([Achleitner *et al.* 2007](#)):

$$V = K.Q_E(t) + K.X.(Q_I(t) - Q_E(t)) \quad (3)$$

where V is the storage within the routing reach (L^3), Q_I is the rate of inflow (L^3/t), Q_E is the rate of outflow (L^3/t), K is a constant equivalent to the time required for a unit discharge wave traveling through the reach (representing prismatic storage), and X is a dimensionless weighting factor that relates to the amount of wedge storage. The storage V varies over time and is approximated by its values at times ($i-1$ and i) ([Achleitner 2008](#)):

$$V = \frac{V_i + V_{i-1}}{2} \quad (4)$$

The Muskingum scheme predicts the outlet flow rate segment as ([Achleitner *et al.* 2007](#)):

$$Q_{E,i} = \frac{Q_{I,i}.C_A + V_{i-1}}{C_B} \text{ where } C_A = \frac{\Delta t}{2} - K.X \text{ and } C_B = \frac{\Delta t}{2} + K.(1 - X) \quad (5)$$

The Muskingum parameter, K , applies to the total reach. When multiple subreaches are present, a reach is split into n equal subreaches, each having an associated Muskingum parameter K' ([Achleitner 2008](#)):

$$K' = \frac{K}{n} \quad (6)$$

Subsequently, Muskingum scheme for each subreach j , considering that $Q_{I,i}^j = Q_{E,i}^{j-1}$, is ([Achleitner 2008](#)):

$$Q_{E,i}^j = \frac{Q_{E,i}^{j-1}.C_A + V_{i-1}^j}{C_B} \text{ where } C_A = \frac{\Delta t}{2} - K'.X \text{ and } C_B = \frac{\Delta t}{2} + K'.(1 - X) \quad (7)$$

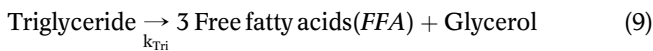
and the total volume in the reach is ([Achleitner 2008](#)):

$$V_i = \sum_{j=1}^n V_i^j \quad (8)$$

The corresponding values for K' , X , and Δt in this study were 300 seconds, 0.1, and 300 seconds, respectively. Depending on the length of the pipe between two inline manholes, the pipe was assigned a number of reaches. Each reach was defined as a 300 ft pipe segment, which was then further divided into three subreaches ($n = 3$). The outflow of one reach would be the inflow of the next one immediately downstream of it. The transport model followed the actual flow pattern of the wastewater in the gravity and force mains where it started from the sources, ended in the treatment plant, and included any existing addition or separation of flow at each manhole. Simulations were performed with an increased number of subreaches (i.e., $n = 4, 5$, and 6) and reduction in the K' , X , and Δt values (i.e., 10 and 20% reduction).

Transport and kinetics of FOG deposit formation

As mentioned earlier, the kinetics of FOG deposits in this study relies on the findings of *Iasmin et al. (2016)*. However, for simplicity, there were some modifications to the kinetics of that study and abrasion of FOG deposits were not considered. In the present study, the hydrolysis rate was simplified to a first order reaction kinetics (Equation (10)), and due to the absence of the intense mixing conditions that were experienced in the lab, the destruction of saponified solids was not considered (Equation (11)). The effects of temperature were also excluded for simplicity. However, significant effects of temperature on the kinetics of FOG deposit formation have been reported in the literature (*Iasmin et al. 2014*).



$$r_{FOGT} = k_{Tri} \times [\text{FOG}] \quad (10)$$



$$r_{SAP} = k_{SAP} \times [\text{Ca}^{2+}] \times [\text{FFA}]^2 \quad (12)$$

where r_{FOGT} and r_{SAP} are the rate of FOG hydrolysis and saponification ($\text{mol}\cdot\text{L}^{-1}\cdot\text{s}^{-1}$), k_{Tri} (s^{-1}) and k_{SAP}

($\text{L}^2\cdot\text{mol}^{-2}\cdot\text{s}^{-1}$) are the hydrolysis and saponification rate constant, and $[\text{FOG}]$, $[\text{Ca}^{2+}]$, and $[\text{FFA}]$ are the concentrations of FOG, calcium, and FFA ($\text{mol}\cdot\text{L}^{-1}$), respectively.

Keener et al. (2008) and later *Iasmin et al. (2014)* stated that FOG deposits have an adhesive character and can become securely bound to interior pipe walls. As a result of this adhesiveness, saponified solids that have formed in the wastewater might be able to aggregate with those solids that have directly formed on the pipe wall. To simulate this effect, an aggregation reaction was also considered (Equation (13)):

$$r_{AGG} = k_{AGG} \cdot \gamma \cdot S_L \cdot S_W \quad (13)$$

where, r_{AGG} is the rate of aggregation ($\text{mol}\cdot\text{L}^{-1}\cdot\text{s}^{-1}$), k_{AGG} is the aggregation affinity constant ($\text{L}\cdot\text{mol}^{-1}$), S_L is the concentration of saponified solids in the liquid phase ($\text{mol}\cdot\text{L}^{-1}$), S_W is the concentration of saponified solids on the pipe wall ($\text{mol}\cdot\text{L}^{-1}$), and γ is the shear rate (s^{-1}), which is computed as $\gamma = (4Q/P \cdot R_h^2)$ with P as the wetted perimeter of the sewer pipe (m) and R_h being the hydraulic radius of the partially full sewer pipe (m).

It was assumed that the solids, S_w , will occupy the interior pipe volume associated with the pipe segment. Therefore, the final wall solids accumulated in any pipe segment was computed by multiplying S_w by the ratio of storage volume, V , divided by the pipe segment volume.

The above kinetics were incorporated into CITY-DRAIN using the transport equations (Equations (14)–(18)). By definition, flows and concentrations exchanged during a time period are considered as mean concentrations over the respective time step Δt (*Achleitner 2008*). The subscripts I (subreach influent) and E (subreach effluent) represent the mean flow and concentrations between t_{i-1} and t_i :

$$\text{FOG: } \frac{d(V \cdot (\text{FOG}))}{dt} = Q_I \cdot [\text{FOG}]_I - Q_E \cdot [\text{FOG}]_E + \{-K_{Tri} \cdot [\text{FOG}]\} \cdot V \quad (14)$$

$$\text{FFA: } \frac{d(V \cdot [\text{FFA}])}{dt} = Q_I \cdot [\text{FFA}]_I - Q_E \cdot [\text{FFA}]_E + \{3K_{Tri} \cdot [\text{FOG}] - 2K_{SAP} \cdot [\text{FFA}]^2 [\text{Ca}]\} \cdot V \quad (15)$$

$$\text{Ca: } \frac{d(V \cdot [\text{Ca}])}{dt} = Q_I \cdot [\text{Ca}]_I - Q_E \cdot [\text{Ca}]_E - \{K_{\text{SAP}} \cdot [\text{FFA}]^2 [\text{Ca}]\} \cdot V \quad (16)$$

$$\text{S}_L: \frac{d(V \cdot [\text{S}_L])}{dt} = Q_I \cdot [\text{S}_L]_I - Q_E \cdot [\text{S}_L]_E + \{K_{\text{SAP}} \cdot [\text{FFA}]^2 [\text{Ca}]\} \\ - k_{\text{AGG}} \cdot \gamma \cdot [\text{S}_L] \cdot [\text{S}_W] \cdot V \quad (17)$$

$$\text{S}_W: \frac{d(V \cdot [\text{S}_W])}{dt} = \{K_{\text{SAP}} \cdot [\text{FFA}]^2 [\text{Ca}] + k_{\text{AGG}} \cdot \gamma \cdot [\text{S}_L] \cdot [\text{S}_W]\} \cdot V \quad (18)$$

Sewer collection system case studies

The formation of FOG deposits was simulated for two sewer collection systems: one in the North East USA and designated as NE, the other in the South West USA and designated as SW. The NE municipality provided information on locations of local restaurants in 2009, average monthly flow rate of wastewater for the duration of two years, geographical information system (GIS) data of the sewer collection system, and a map of reported high FOG deposit accumulation zones that were determined from visual observations. Since FSEs may open and/or go out of business frequently, the geographical data of all FSEs that have been in operation in 2009 were updated. Google map data were used to verify that the FSEs were still in operation. If the FSE was no longer in operation, it was deleted from the list. On the other hand, Google and Google map data were used to add additional FSEs that started operating after 2009 to 2012 (the year this research was performed) to the list. The list of FSE reported in 2009 was called ‘current FSEs’ since the simulation was performed with the data corresponding to year 2009. The map of additional FSEs added after 2009 to the year this research was done (year: 2012) was called ‘new FSEs’. For both current FSE and new FSE scenarios, geographical latitude and longitude of every FSE location were extracted and incorporated into GIS maps.

For the SW model, a map of the urban drainage system containing wastewater flow pattern, locations of FSEs as of 2009, and information on how frequent different pipe

segments were cleaned were provided by the SW municipality. Since the information on when FSEs were in operation in different years was not available for the SW collection system nor was there information about where to add commercial establishments in regions of the collection system that may be zoned for those additions, the new FSEs scenario for SW was defined by randomly reducing the number of current FSEs to half of its original number. A real-world example for this case may be when FSEs have gone out of business and therefore do not discharge FOG waste.

Simulations

FOG deposit formation happens over a three-month to two-year period (Keener *et al.* 2008). However, a 7-day period with 300 seconds interval was chosen to reduce the overall model simulation time.

The wastewater was divided into two major streams for both NE and SW models: BGWW, which represents typical domestic wastewater and contains insignificant FOG concentration, and FSE wastewater (FSE WW) representing the effluent of the grease interceptor from an FSE facility with 200 ppm triglyceride. The calcium concentration was assumed to be identical for both BGWW and FSE wastewater streams and was chosen to be 50 ppm.

For both NE and SW models, the FSE WW flow rate is $6.31 \times 10^{-4} \text{ m}^3/\text{s}$ (10 gal/min), which was taken from a cumulative distribution function for FSE flows at 95% less than the value in Aziz *et al.* (2012).

The NE BGWW flow rate ($0.1503 \text{ m}^3/\text{s}$) was adjusted such that the sum of the BGWW and FSE wastewater flow rate would be equal to the annual average flow provided by the municipality. Assuming a pipe diameter of 0.381 m (equals 15 inches, a frequently used diameter for sewer pipes), the scour velocity for NE sewer collection pipes would be more than 0.762 m/s (2.5 ft/s). This 0.762 m/s (2.5 ft/s) value is the recommended minimum scour velocity used by the wastewater industry to avoid debris deposition in sewer pipes. The SW BGWW flow rate, $0.026 \text{ m}^3/\text{s}$, was calculated using Manning’s equation, a pipe scour velocity greater than 0.762 m/s and a sewer pipe diameter of 0.381 m.

Both NE and SW are local city municipalities with separated sewers. NE has an approximate per capita flow

of $4 \times 10^{-6} \text{ m}^3/\text{s}$ (about 90 gallon per day per capita) while SW has about $3 \times 10^{-6} \text{ m}^3/\text{s}$ (approximately 70 gallon per day per capita). This flow corresponds to the section of the collection system that was modeled.

Determining hotspots and model calibration

Hotspots were defined as locations in the urban drainage system where there is a high rate of FOG deposits' accumulation, and consequently, a potential for an SSO occurrence. The rate of FOG deposits' accumulation was computed based on the time rate of change in the FOG deposit concentration at the wall.

Model calibration was performed by adjusting the saponification reaction rate constants (k_{Tri} , k_{SAP} , and k_{AGG}) such that the model's rate of saponified solids' formation at the wall coincides with sewer system pipe locations where there are high FOG deposit accumulation zones from visual observation or where a high frequency of maintenance was reported by the municipality. A Monte Carlo sampling approach consisting of drawing a random value from a defined probability distribution for all model inputs was performed in this study. A range of values was provided for each rate constant in the saponification model assuming a log normal distribution with an assigned mean value and variance. Initial ranges used for these rate constants were $2.86 \times 10^{-4} \pm 3.54 \times 10^{-4}$ for K_{Tri} , $3.82 \times 10^{-4} \pm 6.31 \times 10^{-4}$ for K_{SAP} , and $2.99 \times 10^{-4} \pm 5.31 \times 10^{-4}$ for K_{AGG} . Wider ranges (50% increase) were also examined and no significant improvement (i.e., less than 5%) in the fitted constants was noted. The equations used to generate the random samples for each distribution are defined in Morgan & Henrion (1990) and are based on the method of inverting the cumulative distribution function (Papoulis 1991). For a 95% confidence interval with a 10% maximum error on the mean value estimate, more than 96 runs should be conducted (Hogg & Tanis 1993). Ninety-eight sets of rate constants, one for each input (k_{Tri} , k_{SAP} , and k_{AGG}), were randomly generated. The three models were simulated with these 98 rate constant scenarios and the rate of change of FOG deposit accumulation at the wall was calculated for each monitoring point in the sewer collection system. The points with the highest rate of FOG accumulation, which consisted of the top 20% of all

monitoring, were compared to pipe segments that were reported to have high FOG deposit accumulation from visual inspection or that required a high frequency of cleaning to remove FOG deposit accumulation.

Twenty percent provided enough locations to compare with the data provided by each of the two sewer collection systems. Higher percentages did not change the performance of the model since 20% covered all the problem areas reported by the two municipalities in the section of the collection system simulated.

Sensitivity analyses

A sensitivity analysis was performed using the data generated from the Monte Carlo statistical method presented in the previous section to investigate the sensitivity of hotspot locations on the selection of k_{Tri} , k_{SAP} , and k_{AGG} . The results of each scenario were then analyzed using Spearman rank correlation to determine the sensitivity of the hotspots to these three rate constants.

Since microbially induced concrete corrosion (MICC) has been recently identified as a potential pathway to FOG deposit formation (He et al. 2013) by releasing significant amounts of calcium, a sensitivity analysis was also performed using 98 randomized values for calcium concentration in FSE wastewater. The values ranged from 50 to 100 ppm. This analysis may show how different rates of MICC at different locations throughout the collection system could impact FOG deposit formation.

Effect of flow variation

For the FSE flow, a peak factor of 6.2 was calculated according to Aziz et al. (2012). The minimum flow was assumed to be zero (Aziz et al. 2012) since there is no FOG waste produced during the times that FSEs are closed (1:00 a.m. to 9:15 a.m.). There are three peak times during the activity of the FSEs: (i) around lunch time (11:30 a.m. to 12:30 p.m.), (ii) around dinner time (8:30 p.m. to 9:30 p.m.), and (iii) when cleaning activities are being performed before closing time (12:00 a.m. to 1:00 a.m.) (Aziz et al. 2012). The FSE flow at all other times was adjusted such that the average flow would match the average value of $6.31 \times 10^{-4} \text{ m}^3/\text{s}$ (10 gal/min).

For NE BGWW, the peak and minimum flow factors were calculated to be 3.5 and 0.3, respectively, based on city population (Qasim 1998). Similarly for the SW BGWW, the peak and minimum flow factors were 2.5 and 0.4, respectively (Qasim 1998). Generally, low municipal wastewater flows occur at night with peak flows during morning and evening periods (Butler & Davies 2004).

RESULTS AND DISCUSSION

Calibration results

The top 20 locations in NE that had the highest rate of saponified solid accumulation were compared to the hotspot locations reported by the municipality. FSE information from 2009 was used in this analysis. Results showed that multiple sets of rate constants generated the highest agreement. When using these rate constants, the model was able to predict 13 out of the top 20 locations that were in agreement with the municipality's reported high FOG accumulating pipe segments (circles with a plus sign in Figure 1). For SW

collection system, the top 20% with the highest rate of FOG deposit accumulation was compared to the reported cleaning frequency of the sewer system. The top 20% represented 14 locations (hotspots), of which 10 hotspots were in agreement with the SW municipality cleaning frequency maps when simulated with the calibrated set of rate constants (circles with a plus sign in Figure 2). The mean and standard deviation of rate constants associated with the best fits for both NE and SW sewer collection system models are as follows: $1.30 \times 10^{-3} \pm 6.01 \times 10^{-4}$ for K_{Tri} , $8.46 \times 10^{-4} \pm 4.70 \times 10^{-4}$ for K_{SAP} , and $1.13 \times 10^{-6} \pm 5.50 \times 10^{-7}$ for K_{AGG} .

The model also predicted hotspot locations that were not reported by the municipality (circles with triangle in Figures 1 and 2), as well as not predicted zones of FOG deposit accumulation that were reported by the municipality (black circles in Figures 1 and 2). The inability of models to predict hotspots reported by the municipality can be due to a number of factors. Pipe deformations such as pipe sags have been shown to preferentially accumulate FOG deposits due to the low flow conditions in the deformed pipe segment (Dominic et al. 2013). Low flow conditions will reduce the ability to wash out any accumulated FOG and transport it further downstream beyond the sag location, thus increasing the possibility of a saponification reaction or attachment to the pipe wall at the pipe sag location (Dominic et al. 2013). Another possible location for FOG deposits' accumulation is where roots intrude into the pipe and obstruct the cross-sectional area (Dominic et al. 2013). The tendency of FOG deposits to accumulate on roots is due to the higher surface area provided by the roots (Dominic et al. 2013) or the occurrence of preferential accumulation of FOG by the roots (Ducoste et al. 2009). Other locations where FOG and FOG deposits may accumulate include wet wells and pump stations (Cox & Cox 2009).

In this research, only non-residential FOG producers were considered. Residential dwellings, specifically in densely populated areas, may have a substantial contribution to producing FOG considering the cooking processes in household kitchens (Ducoste et al. 2009). FOG produced and released to the sewer system by residential contributors can significantly modify wastewater quality and thus change the location of hotspots. The model also assumes that FOG waste released by all FSEs has the same characteristics. Iasmin et al. (2014) have shown that different oil types will result in different FOG deposit formation rates. They also

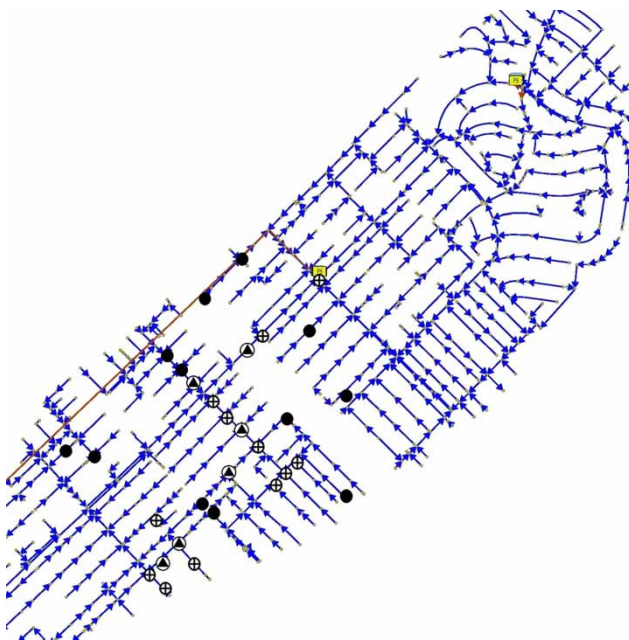


Figure 1 | A section of drainage system in NE with reported and predicted hotspots. Black circles display reported hotspots by the municipality not predicted by the model, circles with a plus sign display hotspots predicted by the model and reported by the municipality, and circles with a triangle show hotspots predicted by the model that were not reported by the municipality.

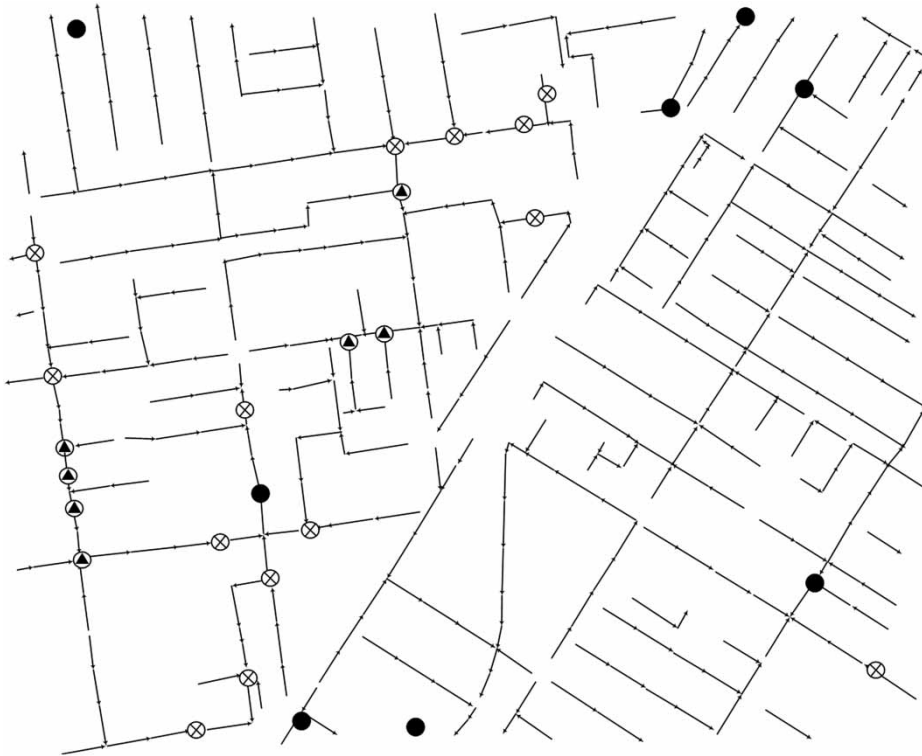


Figure 2 | A section of drainage system in SW with reported and predicted hotspots. Black circles displays reported hotspots by the municipality not predicted by the model, circles with a plus sign display hotspots predicted by the model and reported by the municipality, and circles with a triangle show hotspots predicted by the model and not reported by the municipality.

showed that pH and temperature have a significant influence on the kinetics of FOG deposit formation. In addition, commercial detergents used by FSEs as well as household detergents used by residential communities have been shown to increase the FOG deposit formation rate and quantity due to pH effects as well as surfactants found in these detergents (Iasmin 2014). As discussed in He *et al.* (2013) and Iasmin *et al.* (2014), the extent of concrete corrosion can impact the amount of calcium leaching, which will also have a considerable effect on the saponification rate, especially in older sewer collection systems where corrosion and calcium leaching is of higher concern. Thus, identifying the locations with higher rates of concrete corrosion may improve the accuracy of the model.

Impact of changes in simulation and Muskingum parameters

As mentioned in the Methods section, the corresponding values for K' , X , and Δt in the Muskingum method were

300 seconds, 0.1, and 300 seconds, respectively. Simulations were performed with an increased number of subreaches (i.e., $n = 4, 5,$ and 6) and reduction in K' , X , and Δt values (i.e., 10 and 20% reduction).

For FOG deposit formation period and time steps, simulations of longer than a 7-day period and/or different time steps than 300 seconds displayed no change in the predicted pipe segments with high FOG deposit accumulation rates. Longer simulation periods only changed the amount of FOG deposit accumulation at these high accumulated pipe segments.

Impact of changes in urban landscape

After the models were calibrated using the 2009 FSEs, the effect of changes in the urban landscape was studied by adding or subtracting FSEs from the previously simulated model. For the NE sewer system, comparison was made between model results when simulated with and without these additional restaurants. Results showed that 65%

(13 out of 20 locations) of hotspots were still of high concern after adding the new FSEs (shown with circles with a horizontal line in Figure 3). These locations still represented a high rate of FOG deposit accumulation and have the potential to cause an SSO if left unabated. A possible reason for no change in these 13 hotspots is that some of the new FSEs were located upstream of these locations, and consequently, these locations will experience more FOG discharge.

The other 35% (7 out of 20 locations) of the hotspots were no longer high accumulating zones (circles with a cross sign in Figure 3) and were not among the top 20 locations that had the highest rate of FOG deposit accumulation. In addition to the disappearance of these hotspots, seven new hotspot locations were predicted where there is the potential for a significant amount of FOG deposit accumulation (shown with diamonds in Figure 3). Based on the flow pattern, these locations were all downstream of the newly added FSEs. As discussed in the Methods section, the SW sewer collection system was used to demonstrate the influence of the closure or removal of FSEs on the FOG deposit accumulation in that system.

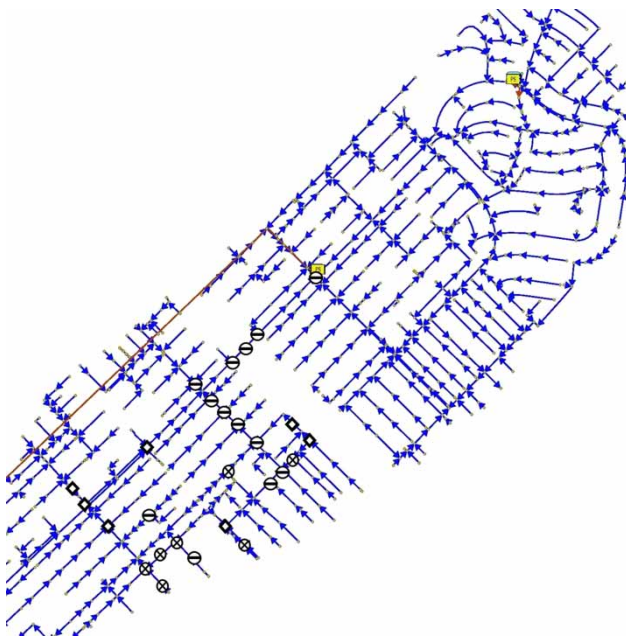


Figure 3 | Effect of adding new FSEs to the NE model. Circles with a horizontal line show hotspots that are still of high concern after adding the new FSEs, circles with a cross sign do not appear to be of high concern anymore, and new locations of high concern are depicted with diamonds.

The steps were similar to those of the NE model. When half of the FSEs were removed from the SW model, most of the previously existing hotspots also disappeared (shown with circles with a cross sign in Figure 4), meaning that those locations no longer posed a high risk of a blockage and potential SSO from FOG deposit accumulation. However, the removal of these FSEs also resulted in new hotspot locations where there is a high risk of FOG deposit accumulation (shown with diamonds in Figure 4). The appearance or disappearance of FOG deposit accumulating zones is critical as the model demonstrates the change in the location where sewer maintenance may be needed due to the change in the number and location of FSEs.

Effect of flow variation

The initial simulations were performed under steady flow conditions. Wastewater discharge may vary depending on the time period of the day. Wastewater from FSEs is also subject to wide fluctuations over time (Aziz et al. 2012). To investigate the influence of transient flow variation, both NE and SW models were simulated with varying FSEWW discharge and BGWW flow patterns (as described in the Methods section) using the calibrated rate constants. Table 1 displays the results in terms of the number of hotspot locations that changed from introducing flow variation.

The modifications in the number of hotspots suggest that the sewer collection system model should include flow variability to completely predict the spatial distribution of locations where there are high risks of FOG deposit accumulation. The effect of these variations may be more significant if seasonal changes are included due to higher peaks and lower minimums.

The impact of flow variation was more significant on the SW collection system compared to the NE collection system. The increased sensitivity to flow variation was due to the difference in the relative distance between the FSEs and the high FOG deposit accumulation zones in SW compared to NE collection systems. For both current and new FSEs in the NE collection system, the majority of the high FOG deposit accumulation zones occur in an area with several FSEs. Many of the new FSEs were also located in this same region and therefore their additional FOG discharge did not change the FOG deposit accumulation location



Figure 4 | Effect of eliminating FSEs from the SW model. Circles with a horizontal line shows hotspots that are still of high concern after adding the new FSEs, circles with a cross sign do not appear to be of high concern anymore, and new locations of high concern are depicted with diamonds.

Table 1 | Number of hotspots that changed due to variable flow rates in NE and SW models

	NE		SW	
	Current FSES	New (Increased) FSES	Current FSES (30 FSES)	Eliminated FSES (15 FSES)
Variable BGWW flow	0	0	6	5
Variable FSE WW	1	3	6	6
Variable BG and FSE WW	1	2	6	5

but did change the rate of formation. In the SW collection system, the FSEs and the resulting hotspots are more widely spread out and hence, the result of variable flow was more significant. However, for both current and eliminated FSES scenarios in the SW collection system, all six locations of hotspots for each variable flow condition are

the same. These SW collection system results suggest that SW may also have an apparent bottleneck location that funnels much of the FOG deposit formation precursors into a specific location.

Sensitivity analysis of FOG deposit formation rate constants and calcium concentration

The results of each scenario from the Monte Carlo approach for NE and SW sewer systems were analyzed using Spearman's rank correlation. Figures S1 to S23 and Tables S1 to S23 in the Supplementary material (available with the online version of this paper) display the distribution and statistical analysis of the variation in the NE collection system, respectively. For both collection systems, the analysis showed that the rate of change of saponified solid accumulation is sensitive to all three rate constants; k_{Tri} , k_{SAP} , and k_{AGG} , with the greatest sensitivity to k_{Tri} , the

rate of FOG hydrolysis, followed by k_{SAP} and k_{AGG} . For the NE collection system with the 2009 FSEs (current FSEs), the correlation coefficients were in the following ranges: 0.1663 to 0.9531 for k_{Tri} , 0.04806 to 0.8662 for k_{SAP} , and -0.0719 to 0.3168 for k_{AGG} . For the SW collection system, k_{Tri} , k_{SAP} , and k_{AGG} were in the range of 0.3414 to 0.8307. The results in Tables S1 to S23 show that all monitored locations are sensitive to the rate constant values with coefficient of variations all higher than 0.4. The distributions of these wall FOG deposit accumulation rates shown in Figures S1 to S23 are primarily skewed to the right, which is similar to the shape of the rate constant distributions. Locations in the sewer collection system with the greatest impact coincided with regions near one of the pump stations in the collection system that pumps the sewer to the treatment plant. One possible reason for the greatest sensitivity to these rate constants in those regions is higher available concentrations of FOG since different pipes connect to a larger inflow pipe to the pump station. This region is also downstream of several FSEs where FOG has had sufficient time to hydrolyze and react with calcium to form deposits.

These results suggest that limiting FOG hydrolysis and the conditions that promote the saponification reaction will have a significant impact on FOG deposit accumulation in the sewer collection system. From a practical standpoint, the mitigation of FOG hydrolysis may be challenging since there may be several pathways that lead to the breakdown of FOG. However, limiting the saponification reaction could be achieved with effective removal of long chain FFA or directing these long chain FFA to undergo alternative chemical reactions so that they are unavailable to react with Ca. Future research should be performed to investigate alternative reactions with long chain FFA or for improving the separation performance of grease interceptors for the removal of FOG and long chain FFA.

The NE collection system model was simulated with 98 different calcium concentrations of FSE wastewater ranging from 50 to 100 ppm, and using the calibrated rate constants. The results were then compared with prior NE collection system simulations with FSE wastewater containing 50 ppm of calcium. Tables S24 to S44 in the Supplementary material (available with the online version of this paper) display the statistical analysis of the locations in the sewer collection system. The results of this sensitivity analysis

showed that the locations of hotspots did not significantly change with the different amounts of calcium in FSE wastewater. As noted by the low coefficient of variation in Tables S24 to S44, the FOG deposit accumulation rates at the wall did not change significantly over the range of calcium concentration simulated. The results of this sensitivity analysis showed that the locations of hotspots did not significantly change with the different amounts of calcium in FSE wastewater. The present model, however, does not capture some of the mechanisms leading to the accumulation of calcium in FOG deposits, i.e., the potential accumulation of calcium in the deposits due to Derjaguin-Landau-Verwey-Overbeek (DLVO) interaction. During saponification, unreacted FFA may be attracted to the saponified solids and be incorporated in the solid matrix. These unreacted FFA likely draw calcium and other cations toward the solid core matrix based on the effects of van der Waals attraction and electrostatic repulsion (i.e., DLVO theory) (He *et al.* 2011, 2013). Another group of researchers suggested that biocalcification may be an alternative mechanism that leads to high calcium levels in FOG deposit samples (Williams *et al.* 2012.) Overall, more measurements and research are needed to prove these different hypotheses.

CONCLUSION

The wastewater collection systems of two cities in the USA (NE and SW) were modeled and simulated using CITY-DRAIN 2.0.3, a MATLAB Simulink model to help assess changes in the wastewater quality in the sewer system due to changes in the urban landscape. Simulations focused on the changes in the quality of wastewater made by the discharge of FOG into the sewers from FSEs. Results of these simulations suggested that a sewer collection system model that incorporates the kinetics and transport FOG chemicals and saponification reactions has the potential to predict many of the FOG deposit accumulating hotspots for a given sewer collection system. While the models were able to demonstrate the impact of spatial changes in the discharge from FSEs on pipe segments with high FOG deposit accumulation, the models did not include important engineering aspects that could influence the outcome of the model predictions. As previously mentioned, pipe deformations such as pipe sags can exacerbate the

accumulation of debris including the accumulation of FOG deposits (Dominic *et al.* 2013). The occurrence of pipe sags may be more prevalent in older sewer collection systems. These Simulink simulations could be enhanced if the hydraulics of these pipe sags were included, where known, in sewer systems. The NE sewer collection system is an older sewer pipe network that contains a significant number of pipe sags where FOG deposit accumulation has been observed. It is possible that unique hydraulic characteristics of these pipe sags could be contributing to the accumulation of FOG deposits and may help explain some of the deviations between the model predictions and the visual observations of FOG deposits' accumulation zones.

In addition, it is likely that different FSEs (i.e., type of restaurant, coffee shop, bakery, etc.) release their wastewater with different FOG and FFA concentrations into the sewer collection system. This concentration variation may occur over hours to days. The current model simulation did not include the impact of spatial concentration discharge variation among the different FSEs in the collection system. Further, the model also did not account for the FSEs to discharge an initial concentration of long chain FFAs. All FFAs produced in the sewer collection system resulted from FOG hydrolysis after FOG discharge from the FSE. To improve the model performance, knowledge of these dynamic changes in FSE wastewater concentration will be important.

Finally, the contribution of non-restaurant and non-fast food FSEs was not considered in the present model. Bakeries, creameries, bars, and coffee shops are just a few other FSEs producing FOG daily. Residential areas are another potential FOG producer and unlike FSEs, are not regulated for discharging waste water containing FOG. By incorporating the above-mentioned missing items into future model development, the results would assist pretreatment managers to plan their future routine maintenances more efficiently, with greater reliability in the model accounting for more existing conditions.

As the urban landscape continues to change with the revitalization of major metropolitan cities, this analysis could be helpful to assess changes in wastewater quality in the sewer system. These hotspot predictions can be performed for any sewer collection system if the necessary GIS data are provided. Predictions from a sewer collection system model that includes

FOG deposit formation kinetics will help assist pretreatment coordinators to plan periodic maintenance schedules and avert detrimental FOG deposit-related SSOs.

ACKNOWLEDGEMENTS

We would like to thank the United States Environmental Protection Agency (EPA STAR grant: 83426401) for funding this research.

REFERENCES

- Achleitner, S. 2008 *Modular Conceptual Modelling in Urban Drainage Development and Application of City Drain*. PhD thesis, Innsbruck University, Innsbruck, Austria.
- Achleitner, S., Möderl, M. & Rauch, W. 2007 *CITY DRAIN© – an open source approach for simulation of integrated urban drainage systems*. *Environmental Modelling & Software* **22** (8), 1184–1195.
- Aziz, T. N., Holt, L. M., Keener, K. M., Groninger, J. W. & Ducoste, J. J. 2012 *Field characterization of external grease abatement devices*. *Water Environment Research* **84** (3), 237–246.
- Brooksbank, A. M., Latchford, J. W. & Mudge, S. M. 2007 *Degradation and modification of fats, oils and grease by commercial microbial supplements*. *World Journal of Microbiology & Biotechnology* **23** (7), 977–985.
- Butler, D. & Davies, J. 2004 *Urban Drainage*. Spon Press, London, UK and New York, USA.
- Canakci, M. 2007 *The potential of restaurant waste lipids as biodiesel feedstocks*. *Bioresource Technology* **98** (1), 183–190.
- Cox, H. W. & Cox, J. 2009 *Treatment of FOG at a Virginia Lift Station Using an Innovative Method*. Innovative Remediation Technologies, Inc. (IRT). http://www.innrt.com/wwtp_files/ESG-12_case_study.pdf (accessed 27 July 2016).
- Dominic, C. C. S., Szakasits, M., Dean, L. O. & Ducoste, J. J. 2013 *Understanding the spatial formation and accumulation of fats, oils and grease deposits in the sewer collection system*. *Water Science & Technology* **68** (8), 1830–1836.
- Ducoste, J. J., Keener, K. M. & Groninger, J. W. 2009 *Fats, Roots, Oils, and Grease (FROG) in Centralized and Decentralized Systems*. WERF Report 03-CT-16T, Water Environment Research Foundation, Alexandria, Virginia, USA.
- Gray, J. 2002 *In A FOG: Wastewater System Managers Struggle with Fat, Oil, and Grease*, Vol. 335. Water Resources Research Institute News of The University of North Carolina, Raleigh, NC, pp. 2–6.
- He, X., Iasmin, M., Dean, L. O., Lappi, S. E., Ducoste, J. J. & de los Reyes, F. L. 2011 *Evidence for fat, oil, and grease (FOG) deposit formation mechanisms in sewer lines*. *Environmental Science & Technology* **45** (10), 4385–4391.

- He, X., de Los Reyes, F. L., Leming, M. L., Dean, L. O., Lappi, S. E. & Ducoste, J. J. 2013 [Mechanisms of fat, oil and grease \(FOG\) deposit formation in sewer lines](#). *Water Research* **47** (13), 4451–4459.
- Hogg, R. V. & Tanis, E. A. 1993 *Nonparametric Methods. Probability and Statistical Inference*. Macmillan Publishing Co., New York, USA.
- Iasmin, M. 2014 *Quantifying Fat, Oil, and Grease Deposits Formation Kinetics*. PhD thesis, North Carolina State University, Raleigh, North Carolina, USA.
- Iasmin, M., Dean, L. O., Lappi, S. E. & Ducoste, J. J. 2014 [Factors that influence properties of FOG deposits and their formation in sewer collection systems](#). *Water Research* **49**, 92–102.
- Iasmin, M., Dean, L. & Ducoste, J. 2016 [Quantifying fat, oil, and grease deposit formation kinetics](#). *Water Research* **88** (1), 786–795.
- Keener, K. M., Ducoste, J. J. & Holt, L. M. 2008 [Properties influencing fat, oil, and grease deposit formation](#). *Water Environment Research* **80** (12), 2241–2246.
- Ma, F. R. & Hanna, M. A. 1999 [Biodiesel production: a review](#). *Bioresource Technology* **70** (1), 1–15.
- Marlow, D. R., Boulaire, F., Beale, D. J., Grundy, C. & Moglia, M. 2010 [Sewer performance reporting: factors that influence blockages](#). *Journal of Infrastructure Systems* **17** (1), 42–51.
- Mattsson, J., Hedström, A., Viklander, M. & Blecken, G. T. 2014 [Fat, oil, and grease accumulation in sewer systems: comprehensive survey of experiences of Scandinavian municipalities](#). *Journal of Environmental Engineering* **140** (3), 04014003.
- Morgan, M. G. & Henrion, M. 1990 *Uncertainty: A Guide to Dealing with Uncertainty in Quantitative Risk and Policy Analysis*. Cambridge University Press, New York.
- Papoulis, A. 1991 *Probability, Random Variables, and Stochastic Processes*. McGraw-Hill, New York, USA.
- Qasim, S. R. 1998 *Wastewater Treatment Plants: Planning, Design, and Operation*. CRC Press, Boca Raton, Florida, USA.
- US EPA 2004 *Impacts and Controls of CSOs and SSOs, Report to Congress*, US Environmental Protection Agency, Washington, DC, USA.
- US EPA 2012 *Controlling Fats, Oils, and Grease Discharges from Food Service Establishments, National Pretreatment Program (40 CFR 403)*. US Environmental Protection Agency, Washington, DC, USA.
- Williams, J. B., Clarkson, C., Mant, C., Drinkwater, A. & May, E. 2012 [Fat, oil and grease deposits in sewers: characterisation of deposits and formation mechanisms](#). *Water Research* **46** (19), 6319–6328.

First received 5 February 2016; accepted in revised form 27 December 2016. Available online 7 March 2017